# Hydromechanical Characterization of Soil-Rockfill Mixtures

Andrea Brito, Ph.D.[1]; Laura Maria Mello Saraiva Caldeira[2]; and João Ribas Maranha[3]

**Abstract:** In order to improve the rather insufficient knowledge about the hydromechanical behavior of soil–rockfill mixtures (SRMs) applied in embankment dams, a testing program was undertaken in which several mixtures with different coarse fractions (CFs) were tested (30, 40, 50, and 70%). SRMs are an environmentally-friendly material that takes advantage of the material excavated for spillways, cut-off trenches, outlet works, and other structures that can be reused. This study presents, for the first time, a systematic experimental program for this type of natural material, involving isotropic and $K_0$ compression tests, undrained triaxial tests, and permeability tests for different CFs. It aims to improve the knowledge about the behavior of this material. All tests performed revealed that SRMs present the same mechanical behavior irrespective of the CF of the mixture. Also, it may be concluded that it is beneficial to add soil to rockfill to constitute an SRM because this results in a stiffer material. **DOI:** **10.1061/(ASCE)MT.1943-5533.0002295.** *© 2018 American Society of Civil Engineers.*

**Author keywords:** Soil–rockfill mixtures; Hydromechanical behavior; Mechanical tests; Permeability tests.



## Introduction

The mechanical and hydraulic behavior of soil–rockfill mixtures (SRMs) is dependent on the fractions of fine and coarse material present in the mixture, the characteristics of the fine fraction (FF), the type and lithology of the rock material, and the maximum particle size (Maranha das Neves 1993). Throughout the construction process and operation phase of the dam, the SRM experiences a change in its grain size distribution, which can result in a change in its properties. In terms of classification, SRMs obey the following conditions (JAE/LNEC 1998): (1) the fraction retained on the 3/4 in. (19 mm) sieve is between 30 and 70%; (2) the fraction passing a #200 (0.074 mm) sieve is between 12 and 40%; (3) and the maximum particle dimension ($D_{max}$) is less than two-thirds of the lift thickness after compaction and not larger than 0.40 m. In this study the coarse fraction (CF), is the fraction of the material retained on the 3/4 in. (19 mm) sieve, and the FF is the remaining fraction.

Over the last 30 years, embankment dam construction has registered a major evolution in Portugal. Environmental and economic issues took on great importance, which has resulted in the incorporation of new materials such as products resulting from excavations and SRMs available in the reservoir area. This has led to a reduction in the transportation costs and environmental impact created by the use of borrow materials outside the area of the reservoir.

[1]Postdoctoral Research Fellow, Geotechnical Dept., Laboratório Nacional de Engenharia Civil, Avenida do Brasil, n° 101, 1700-066 Lisbon, Portugal (corresponding author). Email: andreabrito@lnec.pt

[2]Principal Research Officer, Head of the Geotechnical Dept., Laboratório Nacional de Engenharia Civil, Avenida do Brasil, n° 101, 1700-066 Lisbon, Portugal. Email: laurac@lnec.pt

[3]Research Officer, Geotechnical Dept., Laboratório Nacional de Engenharia Civil, Avenida do Brasil, n° 101, 1700-066 Lisbon, Portugal. Email: jmaranha@lnec.pt

Note. This manuscript was submitted on May 26, 2017; approved on November 29, 2017; published online on April 21, 2018. Discussion period open until September 21, 2018; separate discussions must be submitted for individual papers. This paper is part of the ***Journal of Materials in Civil Engineering***, © ASCE, ISSN 0899-1561.

SRMs have begun to be applied in the shells of several dams, which pose new challenges in estimating the resulting properties of this material in terms of strength, stress-strain behavior, and hydraulic conductivity. Additionally, several of the dams built with this type of material have started to show substantial deformations (Pardo 2006; JAE/LNEC 1991; Caldeira and Brito 2014).

There is a major difficulty in the correct compaction and characterization of such material. An SRM's behavior depends on the relative proportion of its constituents; it approaches soil behavior when the FF is high and the rockfill particles are dispersed in it but approaches rockfill behavior when the coarse particles contact each other and the fine material is in the voids left by them.

Rockfill materials have considerable strength. However, a well-known phenomenon associated with them is collapse by wetting, due to breakage of particles of rock induced by submersion (Terzaghi 1960; Veiga Pinto 1983; Charles 1990a, b; Justo 1991). This phenomenon was detected during one-dimensional compression and triaxial testing on large diameter specimens (Terzaghi 1960; Marsal 1967; Veiga Pinto 1983; Naylor et al. 1986). In recent years, the particle breakage mechanism has been investigated in more detail, and the most important conclusion is that the relative humidity of the particle voids controls the stiffness of coarse-grained materials (Oldecop and Alonso 2001; Chávez and Alonso 2003; Oldecop and Alonso 2007). Also, long-term deformations are caused by particle breakage, rearrangement, and creep (Marsal 1973; Veiga Pinto 1983; Oldecop and Alonso 2001; Alonso and Cardoso 2010). Another important characteristic of rockfill material is that the failure envelope is curved (Charles and Watts 1980; Veiga Pinto 1983; Charles 1990a, b).

In soils, long-term deformations are not important unless they are associated with hydrodynamic consolidation, and the collapse by wetting is small when compared with rockfill materials. Over the past 50 years, critical state models have been used to analyze and explain the behavior of these materials (Roscoe et al. 1958; Schofield and Wroth 1968; Carter et al. 1982; Dafalias 1986; Britto and Gunn 1987; Gens and Potts 1988; Borja and Lee 1990; Been and Jefferies 1985). These models assume that if the soil is subjected to an increasing shear strain, it will reach the critical state.



J. Mater. Civ. Eng., 2018, 30(7): 04018123

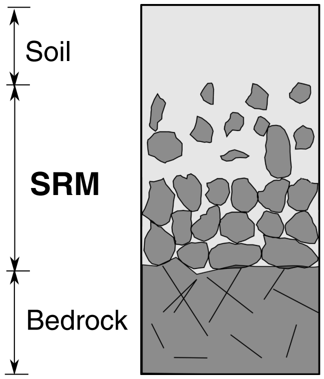


**Fig. 1.** Natural soil, soil-rockfill mixture (SRM), and bedrock profile. (Data from Vallejo and Mawby 2000.)



The most important difference between the two materials for dam applications is the permeability. Rockfill presents a permeability of at least $10^{-5}$ m/s (Maranha das Neves 1993) and consequently a drained behavior in static conditions. Conversely, the permeability of soils shows a strong variation with the type of soil (between $10^{-10}$ and $10^{-3}$ m/s), with the drained or undrained behavior being a function of the loading rate. The failure of both materials is ductile. In fact, in most materials, large plastic deformations occur without complete loss of strength. It is even possible to stabilize them by removing the loading (Maranha das Neves 2002).

The present research aims to determine the aspects of SRMs' behaviors that are similar and dissimilar to those of their constituents—soils and rockfill. This investigation studies natural SRMs obtained by excavation. Fig. 1 shows how these materials occur in nature. In the superficial zone, the engineering properties are only controlled by the soil structure. In the intermediate zone (SRM), the engineering properties are affected by the floating rock particles. Finally, the deeper zone is only controlled by the rock mass. In order to improve the rather insufficient knowledge about the hydromechanical behavior of SRMs, a testing program was undertaken in which several mixtures with different CFs were tested.

## Previous Studies

The study of the behavior of SRMs started earlier, around the 1950s, because of the need to evaluate the stability and deformation of earth–rockfill dams whose bodies contained this material. One of the earliest studies in this field was done by Zeller and Wulliman (1957), who proposed a method of estimating the properties of the material from the results of about 146 triaxial tests on gravelly sand and boulder material. With this purpose, they used materials collected in the Göscheneralp Dam shells in Switzerland and performed triaxial tests on specimens with diameters ranging from 80 to 500 mm in order to establish the relationships between the strength and maximum dimension of the particles. According to the authors, for a given grain-size distribution, the peak shear strength shows a large increase with decreasing porosity.

A second method of estimating the strength was proposed by Lowe in 1964 during the construction of the Shihmen Dam in Thailand. The maximum size of the material used in the dam shells was 304.8 mm and triaxial tests were performed on specimens 152.4 mm in diameter, prepared from a material with a particle size curve parallel to the material placed in the dam. The author introduced the *parallel gradation curve method*. He assumed that if the only difference between the prototype and the specimen is the particle size, the model should reproduce the behavior of the prototype in terms of strength. However, this method has some limitations, including the fact that the surface roughness and breakage of the particles affect the internal friction angle and those properties were not properly modeled using the proposed method (Vallerga et al. 1957). Finally, in some cases the adoption of the parallel gradation curve introduces a considerable fraction of fines that will change the behavior of the material.

In order to investigate the prediction of the internal friction angle of SRMs from tests on smaller samples, Marachi et al. (1969) used the parallel gradation curve method (proposed by Lowe 1964) and performed tests on specimens of three different sizes (914.4, 304.8, and 71.12 mm in diameter) from material obtained from the Oroville Dam. The comparison of the triaxial test results showed that the internal friction angle obtained from the specimen with large particles (maximum particle size of 152.4 mm) was about 3–4° lower than that obtained with the smaller specimen size tested. In addition, it was also noted that the smallest specimen had lower volumetric compression strains than any other tested specimen.

During the construction of the El Infiernillo Dam, Marsal and Rosa (1976) carried out tests on SRMs composed of a CF from basalt in Mexico City with different percentages of soil. Three types of soils were selected: well-graded sand, volcanic silt, and low plasticity clay. The studies concluded that it was beneficial to add granular soil (30–40% of sand) to rockfill because it resulted in a stiffer material. The oedometer tests performed on samples of mixtures with different proportions of clay, silt, and rockfill showed that the compressibility of the mixture was higher than that obtained with rockfill. For percentages of fines larger than 15%, there was a significant reduction in the strength characteristics and an increase of the deformation modulus. For contents of fine material of about 30%, the behavior of the mixture was similar to that of a soil. The study recommended the acceptance of mixtures of rockfill with granular soils (sand or gravel) in a proportion of about 20 to 50% of the total weight in the constitution of dam shells. Conversely, for mixtures with silt or clay, the authors advised that further studies should always be conducted to determine the mechanical properties of the resulting material.

In 1976, Alberro and Marsal proposed conditions for rejecting a soil for an SRM, which are (1) when the soil is expansive, and (2) when the material in the borrow pit has a water content well above the optimum one.

Based on the results of undrained triaxial tests, in 1979, Donaghe and Torrey studied the effect of application of the *scalp-and-replace* method to SRMs. The specimens were compacted at 95% of the standard Proctor test. This study led to the following conclusions:

- SRMs developed large variations in pore pressure under undrained loading;
- Results of the tests performed with the material truncated to the ASTM sieve #4 gave similar results to those obtained with the complete sample in terms of the undrained shear strength;
- The scalp-and-replace method produced conservative effective stress parameters for SRMs;
- For the confining pressure range tested (between 413.7 and 1,379.0 kPa), the results indicated that the internal friction angle decreases with increasing confining pressure; and
- Undrained shear strength obtained in tests carried out on large SRM specimens was considerably higher than that obtained in tests performed on the material fraction passing ASTM sieve #4. The authors noted that this could be attributable to membrane compliance effects.

Iannacchione and Vallejo (2000) studied 31 technical papers containing analysis of shear strengths for clay and sands with varying mixtures of rockfill particles and they concluded that the shear strength gradually increases with increasing percentages of floating particles in unsaturated clays.

In order to investigate the seismic dynamic responses of SRMs at medium loading strain rates, Wang et al. (2017) studied 130 specimens with different coarse fractions. The authors conducted uniaxial compressive strength tests, and they concluded that the rate-dependence characteristic of SRM is strongly influenced by the rockfill in the SRM specimen.

Most of the existing studies are performed with artificial SRMs that have been obtained by mixing rockfill with some type of soil. An example is a study performed by Xu et al. (2009), which carried out large oedometer tests with a mix of broken rock (a limestone) with fine grain soil (Douposi soil). The primary conclusions of the study reveal the significant influence of the fine grains on the compressibility of the mixture, including settlement, creep, and wetting deformation. Another study is presented by Zhang et al. (2016), who studied a SRM obtained by mixing rockfill to a cohesive soil in the construction of the Nuozhadu embankment dam in China. The authors performed large scale in situ load tests and they concluded that rockfill changes the deformation behavior of the ground because the deformation modulus is higher than that of the soil sample. The present study uses SRMs that exist in nature.

## Characterization of SRM

In order to improve the rather insufficient knowledge about the hydromechanical behavior of SRMs, a testing program was undertaken in which several mixtures with different CFs were tested. The materials used in this study came from the shells of Odelouca Dam. It is a zoned embankment dam, 76 m in height, located in Algarve in the south of Portugal. More information about this dam can be found in Caldeira and Brito (2014). The embankment materials include clayey soil in the core and weathered schist and greywacke (SRMs) with a significant fraction of large-sized particles in the shells. The upstream shell incorporates the cofferdam, creating a 14-m-wide berm, at an elevation of 66.50 m.

Due to the fact that the materials used in the construction of Odelouca Dam had a CF generally ranging between 40 and 50% and the limit values for an SRM are 30 and 70%, the mixtures studied had the following CFs: 30, 40, 50, and 70%. Nevertheless, materials with 0% (merely soil) and 100% (purely gravel) CFs were also tested in order to identify the threshold behaviors of the mixture. Fig. 2 shows the grain-size distribution for all SRMs tested after the application of the scalp-and-replace method and using only particles that had passed a 2 in. (50.8 mm) sieve.

### *Index Properties of SRM Fractions*

The material passing the #200 (0.074 mm) sieve has a plasticity index of 12.0% and a liquid limit of 37.3%. According to the Unified Soil Classification System, the fines of the SRMs used in the studies are classified as ML, silt, while the FF is classified as SM, silty sand with gravel. A standard Proctor test was performed on the FF and the optimum point obtained was $\gamma_d^{max} = 19.1$ kN/m$^3$ and $w_{opt} = 12.3\%$.

The tests performed in order to characterize the CF, classified as GP, poorly graded gravel, are very similar to those performed with rockfill material. The rockfill characterization involves three aspects: its structure and lithological composition, its physical and mechanical properties, and its durability. The laboratory tests carried out aimed to determine the physical and mechanical properties and to evaluate the durability of this fraction.

The average values obtained for mass density, dry mass density, saturated mass density, porosity, and water absorption for the $>3/4$ in. material were 2,820, 2,510, 2,383 kg/m$^3$, 12.6, and 5.3%, respectively.

The durability of the CF was assessed by *fragmentability*, *Los Angeles*, and *slake durability* tests. In the fragmentability test, the specimen, with a mass of 2 kg and selected grain size distributions, was compressed within the California bearing ratio (CBR) mold by application of 100 strokes of the normal Proctor test pestle (French Standard NF P94-066, 1992). The coefficient of fragmentability ($FR$) is the ratio between the effective diameter

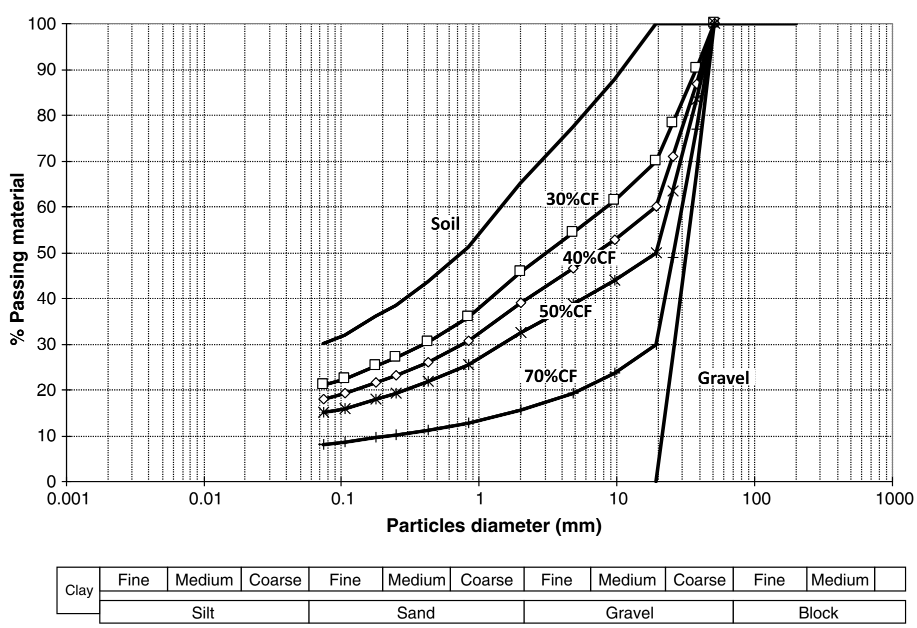


**Fig. 2.** Grain size distribution for SRMs, soil, and gravel studied.

(corresponding to 10% passing material) of the specimen before and after compression. The result obtained for $FR$ was equal to 1, so the gravel specimen had no evolution of the effective diameter after 100 strokes and is not sensitive to this type of action. The Los Angeles test is intended to determine the wear loss (as a percentage) of aggregates with a particle size selected. The test followed the Portuguese Standard NP EN 1097-2 (Portuguese Standard 2002). The wear value obtained was 46%, which is very high, proving that the material is very sensitive to abrasion. The *slake durability index* is obtained by following the ASTM D4644 (ASTM 2016) procedure and is generally defined as the ratio of the weight of the dry specimen retained in a drum after the second test cycle ($Id_2$) of wetting and drying to the initial dry weight of the specimen. However, when the value of $Id_2$ is greater than 90%, it is recommended to be replaced by the value corresponding to the first wear cycle ($Id_1$). In rockfill of moderate to high strength, wear is usually very low, so it is common to use the result corresponding to the seventh wear cycle ($Id_7$; Delgado Rodrigues 1986; Monteiro and Delgado Rodrigues 1994). For this material, the following values were obtained: $Id_1 = 95.96\%$, $Id_2 = 93.85\%$, and $Id_7 = 86.00\%$.

The *crushing strength test* of each sample was performed according to the method proposed by Marsal (1969) for several dimensions of rockfill particles (usually 12.5, 25, and 50 mm). The test consists of placing three particles of approximately equal size between two steel plates, actuated by a loading frame. The upper plate is connected to a dynamometric ring to record the load. The loading frame applies an increasing vertical force distributed by the three particles, arranged in such a way as to better standardize the transmission of the load, until one of these particles is crushed. When this occurs, the value of applied force—the crushing strength ($P_a$)—is recorded. The crushed particle is removed and replaced with a new particle, and the procedure is repeated. For this material, the crushing strength for a theoretical particle size of 50 mm was $P_a50 = 5.7$ kN.

A study performed at LNEC (Veiga Pinto and Prates 1997) defines three strength classes for the most common lithologic types of rockfill: greywacke, limestone, and granite. They are allocated to these classes based on the porosity ($n$), dry unit weight ($\gamma_{dg}$), simple compression strength ($\sigma_c$), point load test parameter ($PLS$), crushing strength for a theoretical particle size of 50 mm ($P_a50$), percentage of wear determined by the Los Angeles machine ($LA$), slake durability index ($Id_7$), and fragmentability index ($FR$). Table 1 presents such a classification for greywacke rockfill. The parameters of a material belonging to Class 1 must comply with all the values prescribed for this class in Table 1. Parameters of materials of Class 2 must have values corresponding to Classes 1 or 2. A material of Class 3 must have at least one parameter with values corresponding to this class. Rockfill of Classes 1 and 2 remain as rockfill materials after construction and during the operation phase. In contrast, rockfill materials of Class 3 tend to evolve into SRMs due to construction and operation actions.

According to the results found, the CF studied is moderately porous, with a low crushing strength, low fragmentability, high sensitivity to abrasion, and resistance to wetting and drying cycles. Given the values obtained in terms of porosity, dry density, crushing strength, and Los Angeles wear, this fraction is included in Class 3 (according to Table 1) and is typically classified as an SRM.

**Table 1.** Classification of greywacke rockfill

| Parameter | Class 1 | Class 2 | Class 3 |
|---|---|---|---|
| $n$ (%) | 1–3 | 3–6 | **6–10** |
| $\gamma_{dg}$ (kN/m$^3$) | 26.5–27.5 | 25.5–26.5 | **24.0–25.5** |
| $\sigma_c$ (MPa) | 130–170 | 90–130 | 50–90 |
| $PLS$ (MPa) | 9–12 | 6–9 | 2–6 |
| $P_a50$ (kN) | 14–18 | 8–14 | **4–8** |
| $LA$ (%) | 15–30 | 30–40 | **40–50** |
| $Id_7$ (%) | **0.5–1.0** | 1.0–1.5 | 1.5–4.0 |
| $FR$ | **1–3** | 3–5 | 5–7 |

Note: The bold values are the intervals which contains the index properties of the material studied.
Source: Data from Veiga Pinto and Prates (1997).

**Table 2.** Vertical saturated hydraulic conductivity for all materials tested

| Sample | $k_V$ (m/s) |
|---|---|
| Soil | $9.5 \times 10^{-10}$ |
| 30% CF | $2.1 \times 10^{-10}$ |
| 40% CF | $4.0 \times 10^{-10}$ |
| 50% CF | $5.0 \times 10^{-10}$ |
| 70% CF | $9.9 \times 10^{-6}$ |
| Gravel | $3.3 \times 10^{-5}$ |

## Tests Performed in Triaxial Apparatus

The specimen dimensions used in the triaxial apparatus are about 230 mm in diameter and 450 mm in height. Each specimen is prepared by the vibrating compaction of about eight layers near the optimum point of the standard Proctor test, taking into consideration the compaction parameters previously obtained on the basis of vibratory tests (Caldeira and Brito 2014).

## Hydraulic Conductivity

After saturation of specimens through the application of a sufficient backpressure to reach values of the Skempton parameter $B$ above 0.95, the saturated hydraulic conductivity was determined in the vertical direction. The results (Table 2) presented a baseline of about $10^{-10}$ m/s for the SRMs with CFs equal to or less than 50% and a baseline of about $10^{-5}$ m/s for 70% CF. The hydraulic conductivity values of the FF (soil) and of the CF (gravel) are, respectively, slightly larger than those of SRMs with CF between 30 and 50% and larger than that of the SRM with CF equal to 70% (with an initial fines content of around 8%; see Fig. 2), reflecting their initial specific volumes and fines contents.

Given the reduced permeability of the materials, the saturation and consolidation phases proved to be quite time consuming for the mixtures with high percentages of fine material. As expected, the mixture of 70% CF took less time because it did not generate as much excess pore pressure during the increase of the cell pressure.

## Compressibility Tests

### Isotropic Compression Tests

To define the slopes of the normal compression line ($\lambda$) and the swelling line ($\kappa$) of the different mixtures, isotropic compression tests were performed with unloading and reloading cycles. Fig. 3 presents the results for all SRMs tested, together with those of the FF (0% CF, soil) and CF (100% CF, gravel), in terms of specific volume versus the mean effective stress logarithm. The SRMs showed the same type of curve and the values obtained for the parameters of the normal compression and swelling lines (included in Table 3) are very similar. The two extreme materials (0 and 100% CF) presented larger values of $\lambda$ and $\kappa$ than the mixtures.



J. Mater. Civ. Eng., 2018, 30(7): 04018123

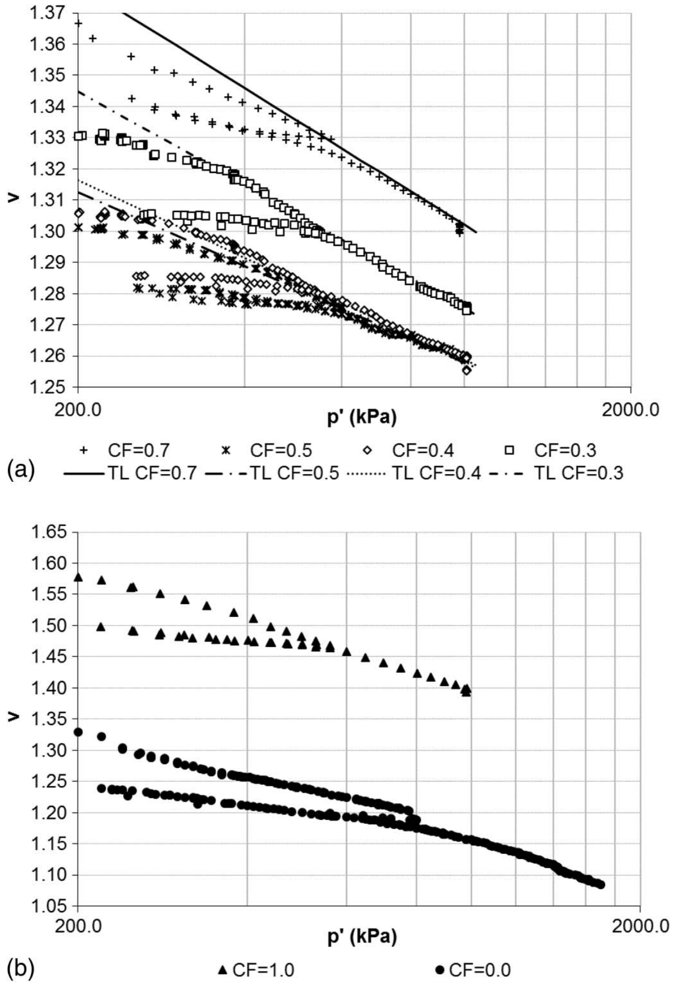


**Fig. 3.** Isotropic compression test results ($v$ versus $p'$) for (a) SRMs and theoretical normal compression lines; and (b) soil and gravel.

**Table 3.** Parameters of the normal compression and swelling lines and the yield stress for all materials tested

| Sample | $N$ | $\lambda$ | $\kappa$ | $\lambda/\kappa$ |
|---|---|---|---|---|
| Soil | 1.728 | 0.079 | 0.022 | 3.6 |
| 30% CF | 1.573 | 0.043 | 0.009 | 4.8 |
| 40% CF | 1.509 | 0.037 | 0.008 | 4.6 |
| 50% CF | 1.490 | 0.033 | 0.009 | 3.7 |
| 70% CF | 1.633 | 0.048 | 0.017 | 2.8 |
| Gravel | 2.258 | 0.125 | 0.038 | 3.3 |

These results allow the following expressions to be deduced:

$$N = 2.7767\ \mathrm{CF}^2 - 2.6314\ \mathrm{CF} + 2.1139(R^2 = 0.9998) \quad (1)$$

$$\lambda = 0.2904\ \mathrm{CF}^2 - 0.2791\ \mathrm{CF} + 0.1009(R^2 = 0.9889) \quad (2)$$

$$k = 0.1\ \mathrm{CF}^2 - 0.08\ \mathrm{CF} + 0.024(R^2 = 1.0) \quad (3)$$

Fig. 3(a) represents the theoretical lines obtained for each mixture based on Eqs. (1) and (2). At low effective mean stresses, the normal compression lines (NCLs) of the SRMs reach lower specific volumes than the soil and gravel materials, which might be explained by the dissemination of coarse particles in the soil at low CF values or by the infilling of voids of the coarse particles with the FF at high CF values. In terms of specific volume, 40% CF and 50% CF mixtures present lower values than the 30% CF mixture because of the presence of more coarse particles completely embedded in the soil. Fig. 4 represents Eqs. (2) and (3).

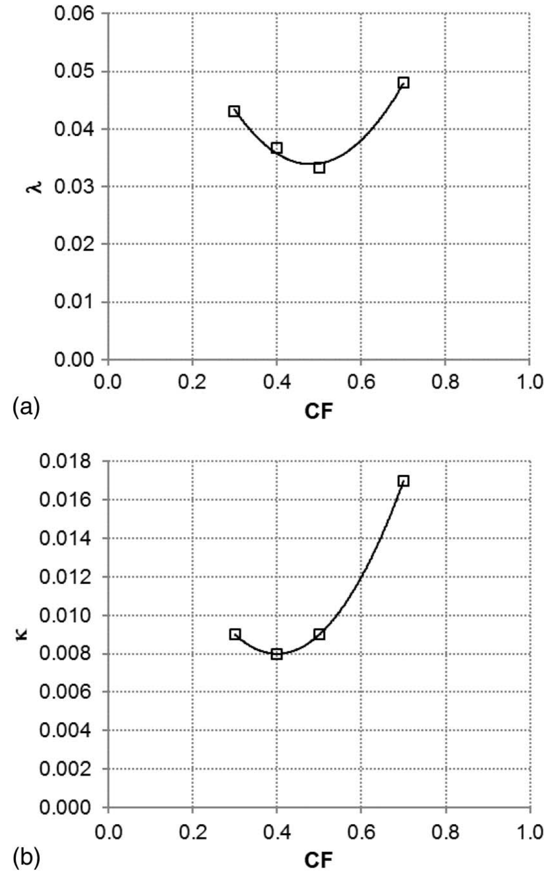


**Fig. 4.** (a) Slope of the normal compression line versus coarse fraction; and (b) slope of the swelling line versus coarse fraction.

The $\lambda$ value of the soil (0% CF) is of the same order as those obtained for decomposed granite (Coop and Lee 1993; Santucci et al. 1998) or residual soil derived from Botucatu sandstone (Martins et al. 2001) composed of sand (70%) and kaolinite (30%). The effect of the CF on SRMs is flattening of the NCL, which increases their stiffness. As the CF of the SRMs is increased, $\lambda$ tends to initially decrease before increasing again at higher CFs, presenting a minimum value when the CF is around 48%. This means that a FF of 52% is just sufficient to occupy the spaces between the coarse particles and will effectively contribute to the behavior. The increase of the gradient of the NCL observed for the gravel (100% CF) is generally believed to correspond to particle damage and can be correlated with the strength of individual particle and number of contacts per particle, which is small given the poorly graded nature of this material (Coop and Lee 1993).

Relative to the slope of the swelling line, the values obtained are almost constant (around 0.008) for SRMs with CFs of between 30 and 50% but almost double for the coarsest mixture (70% CF). Note that another effect of the CF is that it reduces the $\lambda/\kappa$ ratio monotonically.

## $K_0$ Compression Tests

The $K_0$ compression tests were performed with 40 and 70% CFs for evaluation of the coefficient of earth pressure at rest of this type of material. A triaxial apparatus controlled by a software application

**Fig. 5.** Triaxial specimen with three local displacement potentiometers.

specially developed at the LNEC Scientific Instrumentation Centre was used. This software employs direct reading of the specimen diameter to control the axial load when applying radial stress to keep the diameter unchanged with a tolerance of 0.001 mm. Fig. 5 shows the specimen with the three local displacement potentiometers (at the top, middle, and bottom of the specimen) for measuring its diameter. Only the potentiometer in the middle of the sample was used to control the load frame. The others allow the boundary effects and the nonuniform lateral deformation of the specimen to be confirmed. To ensure drained conditions, the rate of application of radial stress was reduced (0.02 kPa/min).

Fig. 6 presents the results in terms of $v$ versus the mean effective stress logarithm for the two mixtures tested (40 and 70% CFs). The slopes of the normal compression line obtained in these tests are $\lambda_{(\mathrm{CF}=0.4)} = 0.035$ and $\lambda_{(\mathrm{CF}=0.7)} = 0.041$, in good agreement with those obtained in the isotropic compression test (presented in Table 2). The differences can be attributed to the nonuniform deformation of the specimen during the $K_0$ compression test. The values of $K_0$ were calculated using the expression

$$K_0 = \frac{3 - \eta_0}{2\eta_0 + 3} \tag{4}$$

where $\eta_0$ represents the stress path slope. Based on these results, the coefficient of earth pressure is equal to 0.401 for the 40% CF mixture and 0.361 for the 70% CF mixture. The soil presented a $K_0$ value of 0.525. As expected, $K_0$ decreases with the increase of the CF, reflecting the effect of the shear strength.

## Undrained Triaxial Tests

Three specimens of each SRM were consolidated under the following confining stresses: 200, 400, and 800 kPa. The value selected for the displacement rate was 0.11 mm/min during the shear phase. Fig. 7 presents, as an example, the results in terms of deviatoric stress and excess pore water pressure as a function of the axial strain and the effective stress paths for all mixtures tested at a confining stress of 400 kPa. All specimens show similar behavior regardless of the applied confining stress. Concerning the shear stress-strain behavior, this figure shows a gradual increase in the deviatoric stress, even after an axial strain of 10%. During the shearing process, excess pore water pressures are generated until a peak is reached (associated with axial strains ranging from 2.3 to 3.3%) and then decrease monotonically. As a consequence, the effective stress paths show an inversion in direction and the material exhibits a gradual transition in stiffness from elastic to elastoplastic behavior. The comparison of different SRMs' behaviors reveals that the higher the values of the deviatoric stress, the lower the generation of excess pore water pressure. In terms of the maximum deviatoric stress, which is a function of the specific volume before shearing, the specimens can be sorted in ascending order as follows: 40, 30, 50, and 70% CF. The peak strength and the strength of the specimens at the end of the tests increase with increasing CF.

Several studies have concluded that the rockfill failure envelope is curved (Charles and Watts 1980; Veiga Pinto 1983; Charles 1990a, b). One of the expressions used for this envelope is the following (Charles 1990a):

$$q_f = a p_f'^b \tag{5}$$

where $q_f$ = deviatoric stress at failure; $p_f'$ = corresponding mean effective stress; and $a$ and $b$ = constants. For soils, $a$ is the parameter $M = q_f/p_f'$ and $b$ is equal to 1. For all SRMs, the failure

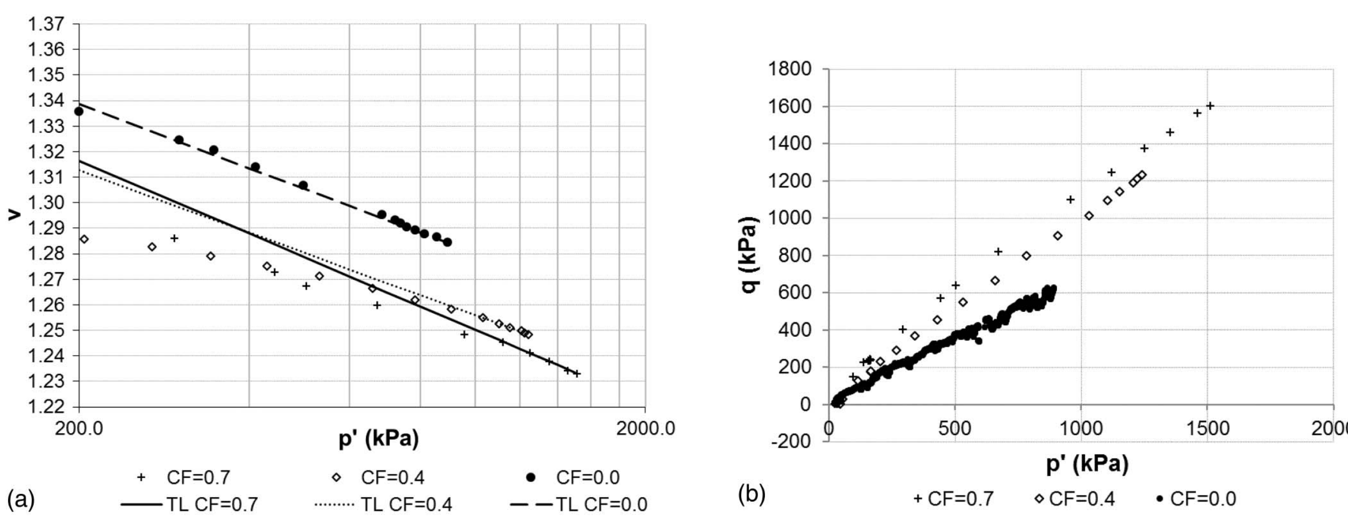


**Fig. 6.** $K_0$ compression tests: (a) $v$ versus $p'$; and (b) effective stress paths.

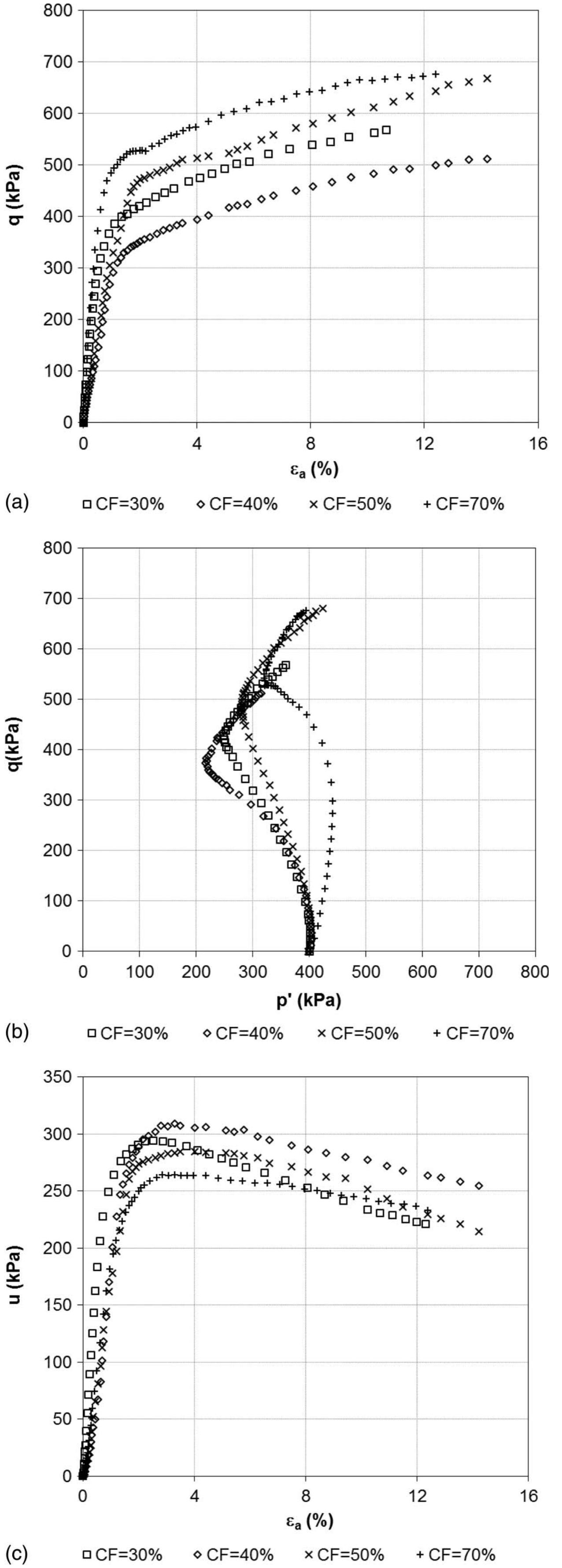


**Fig. 7.** Undrained triaxial compression test for SRMs at a confining pressure of 400 kPa: (a) deviatoric stress versus axial strain; (b) effective stress paths; and (c) excess pore water pressure versus axial strain.

**Table 4.** Constants a and b of the failure envelope for all materials tested

| Sample | *a* | *b* |
|---|---|---|
| Soil | 1.024 | 1.000 |
| 30% CF | 2.715 | 0.903 |
| 40% CF | 4.355 | 0.833 |
| 50% CF | 4.812 | 0.819 |
| 70% CF | 5.279 | 0.846 |
| Gravel | 3.349 | 0.884 |

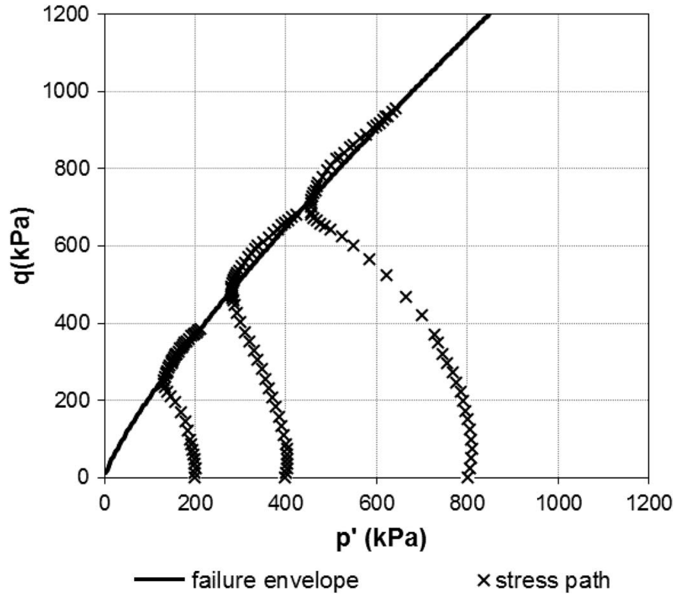


**Fig. 8.** Stress paths and failure envelope for SRM with 50% CF.

envelope that best fits the results is curved and the values of their constants are included in Table 4. All failure envelopes cross the origin, so the cohesion is considered to be zero. Fig. 8 contains the stress paths and the adjusted failure envelope obtained for the SRM with a CF of 50%. Fig. 9 shows a comparison of the failure envelopes and the equivalent friction angles as a function of the mean effective stress at failure of all SRMs with those obtained for the FF (soil) and CF (gravel). The equivalent friction angle was calculated based on the stress ratio ($\eta_f = q_f/p'_f$) at different points of the failure envelope.

It can be observed that the SRMs' failure envelopes are almost coincident. The effect of the CF in SRMs is a considerable increase in the shear strength, which reaches values close to those observed for the CF. The equivalent friction angle decreases with the increase of the mean effective stress for all SRMs and gravel, which is generally explained by the breakage of the coarse particles in rockfill. It also increases with the increase of the SRMs' CF, although only slightly for CFs between 40 and 70%. Nevertheless, the SRMs' behavior in terms of equivalent friction angle is distinctive from that of the gravel, given that it seems to converge to the same value at high mean effective stresses. With the exception of the 30% CF mixture, SRMs also present a large variation of the equivalent friction angle (about 10° for an SRM with a CF of 70%) in the range of stresses studied.

Several factors influence the particle breakage (Lee and Farhoomand 1967; Hardin 1985; Murphy 1970; Billam 1971; Lo and Roy 1973). The amount of particle crushing is affected by the



J. Mater. Civ. Eng., 2018, 30(7): 04018123

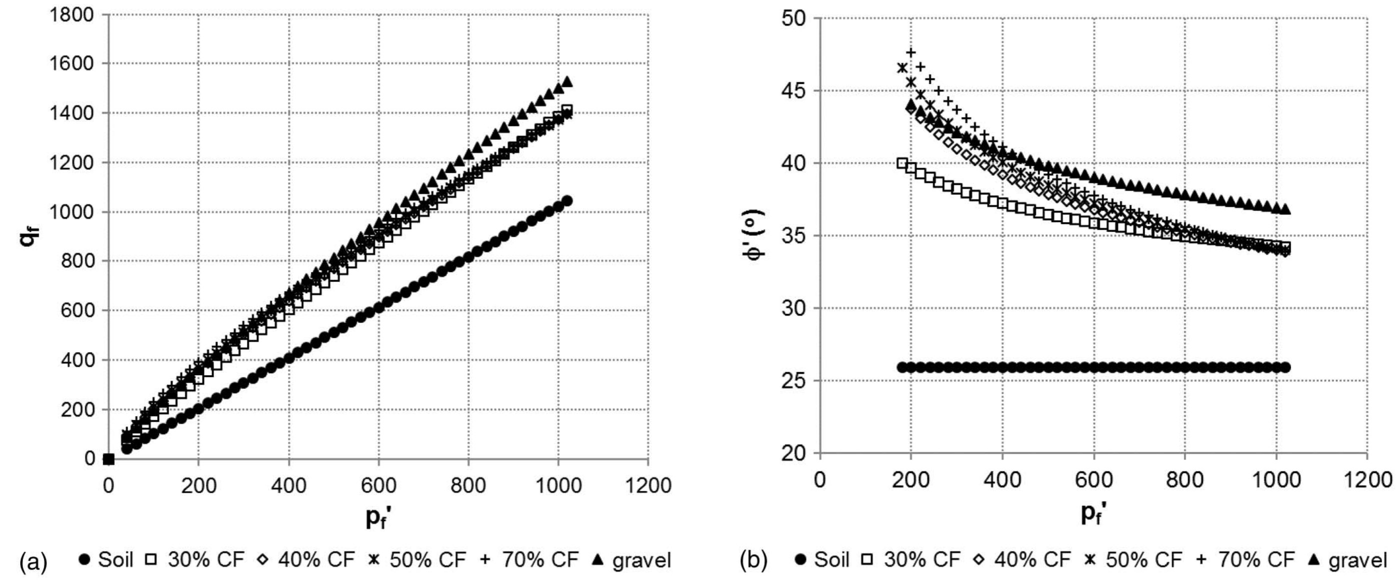


**Fig. 9.** (a) Failure envelopes; and (b) equivalent friction angle as a function of the mean effective stress at failure for all SRMs, fine fraction (soil), and coarse fraction (gravel).

stress level, stress path, particles size, and time (Lade et al. 1996). The time effect is discussed in detail by Yamamuro and Lade (1993). McDowell and Bolton (1998) associated the linear compression line of crushable soils to the evolution of a fractal distribution of particles size. Several authors (Cundall and Strack 1979; McDowell and Harireche 2002; McDowell and Bono 2013) used discrete element methods to investigate size effects and the micromechanics of one-dimensional compression of aggregates.

To assess the influence of breakage on the behavior of SRM*s* and gravel, the grain size distribution before and after each triaxial test was determined. Fig. 10 shows these results for the triaxial tests performed at an effective confining stress of 800 kPa, where the grain size evolution is clear and is caused by specimen preparation (compaction), isotropic compression, and the application of deviatoric stresses.

To characterize the grain size evolution of rockfill, Marsal (1973) proposed a breakage parameter equal to the sum of the positive differences between the percentage of the total sample comprised by each grain size fraction before and after testing. This parameter takes into account the fragmentation process of all fractions. This parameter was determined for all SRMs and CFs. Fig. 11(a) presents the breakage parameter as a function of the confining stress for these materials. The breakage process is more pronounced for the mixtures with more coarse material and for the highest confining stress due to the reduced number of contacts between particles and high forces transmitted at these contact points.

The presence of a large FF (30% CF) with the coarse particles dispersed in it makes the crushing practically independent of the loading history, reducing the initial CF to less than 5% and

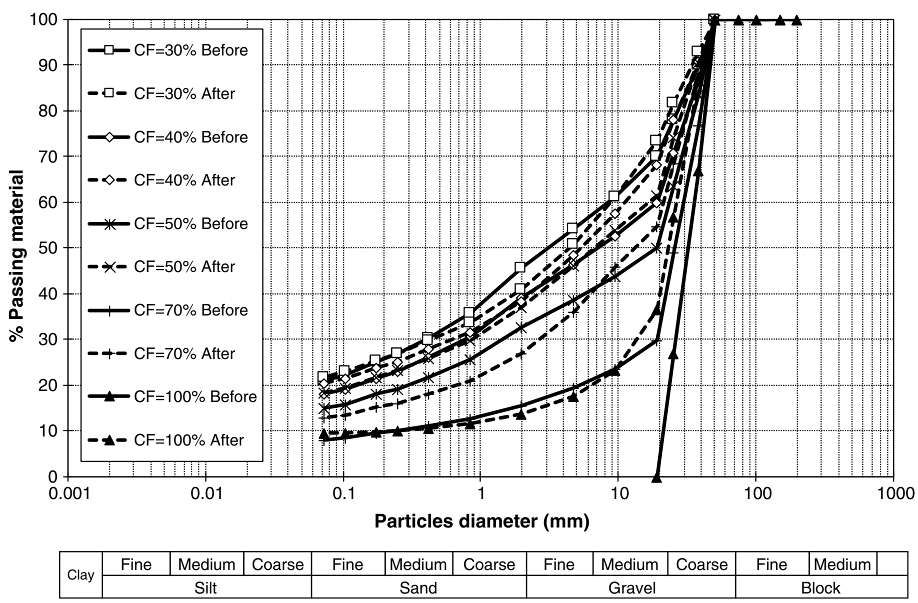


**Fig. 10.** Grain size distribution before and after triaxial tests for all SRMs and gravel at a confining effective stress of 800 kPa.

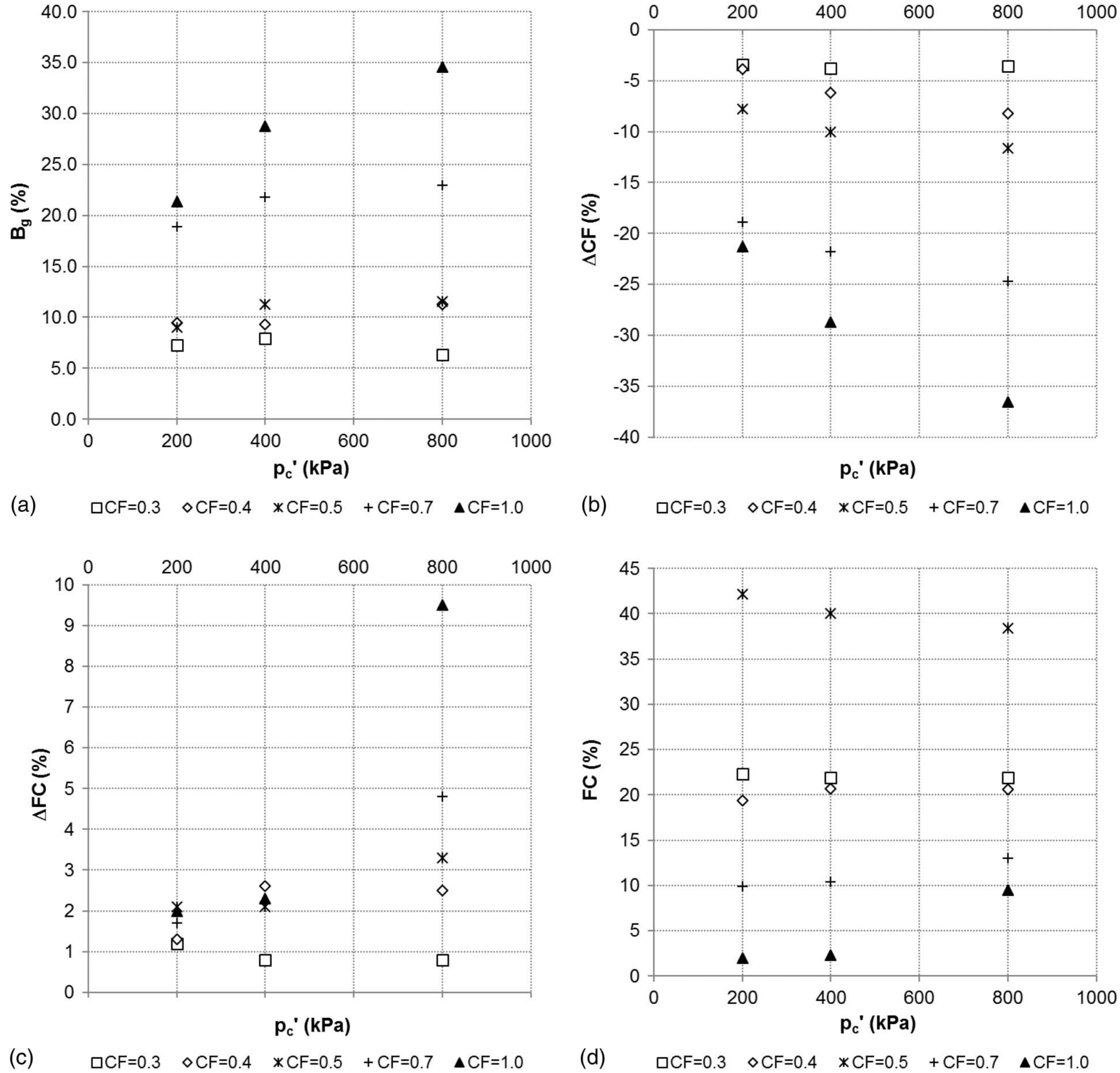


**Fig. 11.** (a) Grain breakage factor ($B_g$); (b) variation in coarse fraction (ΔCF); (c) fine contents variation (ΔFC); and (d) fines content (FC) as a function of the confining stress after triaxial tests.

generating a minor increase of fines particles (about 1%). It seems that the breakage phenomenon is especially associated with the compaction process. In contrast, when the FF is small (70% CF) or nonexistent (100% CF), the crushing of the CF is significant and dependent on the loading history, with the breakage parameter ranging between 19 and 23% for the 70% CF mixture and between 21 and 35% for the gravel when the confining stress varies between 200 and 800 kPa.

Above all, the crushing influences the CF, whose variation is shown in Fig. 11(b), is practically symmetrical to Fig. 11(a). The decrease of the CF increases with increases in the initial CF and increases in the confining pressure ($p_c'$), presenting a logarithmic variation with $p_c'$ for all materials with CFs larger than 30%, which can explain the curved shape of the envelope. The increase in the fine contents is generally small, as shown in Fig. 11(c), except for the highest confining stress.

Another aspect that is important to mention is that the material with a CF of 70% is only considered an SRM for the largest confining stress, where the fines content is higher than 12%. This explains the high value of saturated hydraulic conductivity determined for this material, which is very close to that obtained for the gravel.

For normally consolidated soils, Jacky (1948) and Brooker and Ireland (1965) proposed empirical correlations between the values of $K_0$ and the internal friction angle in terms of effective stresses, $\phi'$, of the following type:

$$K_0 = d - \sin\phi' \tag{6}$$

where $d$ is the empirical constant. Based on $K_0$ and the internal friction angle for the high confining stress values (800 kPa) previously obtained, the empirical constants are $d_{(CF=0.0)} = 0.96$, $d_{(CF=0.4)} = 0.98$, and $d_{(CF=0.7)} = 0.93$, of which the first and second are in the range proposed by Jacky (1948) ($d = 1$), and Brooker and Ireland (1965) ($d = 0.95$) for soils, with the empirical constant being slightly lower for the SRM with a CF of 70%.

## Conclusions

To characterize the hydromechanical behavior of natural SRMs, a testing program involving the determination of the index properties of SRM fractions and the use of triaxial apparatus was undertaken. The FF can be classified as silt with gravel and sand, while the CF can be classified as poorly graded gravel, which tends to evolve into an SRM. The saturated hydraulic conductivity presented a reference point of about $10^{-10}$ m/s for the SRMs with CFs equal to or less than 50% and a reference point of about $10^{-5}$ m/s for 70% CF. The results of the isotropic consolidation tests show that the effect of the CF on SRMs is a decrease in the initial specific volume ($N$) and flattening of the NCL. $\lambda$ tends to initially decrease before increasing again with higher CFs, presenting its minimum value when the CF is around 48%. It may be concluded that it is beneficial to add soil to rockfill to form an SRM because this results in a stiffer material. The slopes of the normal compression line obtained in $K_0$ compression tests are in good agreement with those obtained in the isotropic compression test, and $K_0$ decreases with the increase of the CF, reflecting the effect of shear strength. The SRMs' failure envelopes are curved and almost coincident. The effect of the CF is a considerable increase in the shear strength. The equivalent friction angle decreases with the increase of the mean effective stress, which is explained by the breakage of the coarse particles, and converges to the same value at high mean stresses.

Empirical correlations between the values of $K_0$ and the internal friction angle in terms of effective stresses for high confining stress were established and were similar to those proposed by Jacky (1948) and Brooker and Ireland (1965).

## Acknowledgments

The authors would like to acknowledge the owner of Odelouca Dam, Águas do Algarve, SA, for making the materials available for the tests. We would also like to express our gratitude to the LNEC technicians for their contribution to the experimental work. The financial support provided by FCT (the Portuguese Foundation for Science and Technology) to the first author under Ph.D. Grant No. SFRH/BD/87315/2012 is gratefully acknowledged.

## References

Alberro, J. A., and R. J. Marsal. 1976. "Earth and rockfill dams." In Vol. 1 of *Trans. 12th Int. Congress Large Dams*, 538–571. Paris: ICOLD.

Alonso, E. E., and R. Cardoso. 2010. "Behavior of materials for earth and rockfill dams: Perspective from unsaturated soil mechanics." *Front. Archit. Civil Eng. China.* 4 (1): 1–39. https://doi.org/10.1007/s11709-010-0013-6.

ASTM. 2016. *Standard test method for slake durability of shales and other similar weak rocks*. ASTM D4644. West Conshohocken, PA: ASTM.

Been, F. G., and M. G. Jefferies. 1985. "A state parameter for sands." *Géotechnique.* 35 (2): 99–112. https://doi.org/10.1680/geot.1985.35.2.127.

Billam, J. 1971. "Some aspects of the behavior of granular materials at high pressures." In *Proc., Roscoe Memorial Symp.*, 69–80. Oxford, UK: G.T. Foulis.

Borja, R. I., and S. R. Lee. 1990. "Cam clay plasticity. Part I: Implicit integration of elasto-plastic constitutive relations." *Comput. Methods Appl. Mech. Eng.* 78 (1): 49–72. https://doi.org/10.1016/0045-7825(90)90152-C.

Britto, A. M., and M. J. Gunn. 1987. *Critical state soil mechanics via finite elements*. Chichester, UK: Ellis Horwood.

Brooker, E. W., and H. O. Ireland. 1965. "Earth pressures at rest related to stress history." *Can. Geotech. J.* 2 (1): 1–15. https://doi.org/10.1139/t65-001.

Caldeira, L., and A. Brito. 2014. "The use of soil–rock mixtures in dam construction." *J. Constr. Eng. Manage.* 140 (8): 04014030. https://doi.org/10.1061/(ASCE)CO.1943-7862.0000864.

Carter, J. P., J. R. Booker, and C. P. Wroth. 1982. "A critical state soil model for cyclic loading." In *Soil mechanics–transient and cyclic loads*, edited by G. N. Pande and O. C. Zienkiewicz 219–252. New York: Wiley.

Charles, J. A. 1990a. "Laboratory compression tests and the deformation of rockfill structures." *Chap. 4 in Advances in rockfill structures*, 53–72. Dordrecht, Netherlands: Springer.

Charles, J. A. 1990b. "Laboratory compression tests and the deformation of rockfill structures." *Chap. 5 in Advances in rockfill structures*, 73–96. Dordrecht, Netherlands: Springer.

Charles, J. A., and K. S. Watts. 1980. "The influence of confining pressure on the shear of compacted rockfill." *Geotechnique.* 30 (4): 353–367. https://doi.org/10.1680/geot.1980.30.4.353.

Chávez, C., and E. E. Alonso. 2003. "A constitutive model for crushed granular aggregates which includes suction effects." *Soils Found.* 43 (4): 215–227. https://doi.org/10.3208/sandf.43.4_215.

Coop, M. R., and I. K. Lee. 1993. "The behavior of granular soils at elevated stress." In *Proc. Wroth Memorial Symp.—Predictive Soil Mechanics*, edited by G. T. Houlsby and A. N. Schofield, 101–112. London: Thomas Telford.

Cundall, P. A., and O. D. L. Strack. 1979. "A discrete numerical model for granular assemblies." *Géotechnique.* 29 (1): 47–65. https://doi.org/10.1680/geot.1979.29.1.47.

Dafalias, Y. F. 1986. "Bounding surface plasticity I: Mathematical foundation and hypoelasticity." *J. Eng. Mech.* 112 (EM9): 966–987. https://doi.org/10.1061/(ASCE)0733-9399(1986)112:9(966).

Delgado Rodrigues, J. 1986. *Contribuição para o estudo das rochas carbonatadas e sua classificação geotécnica*, 1–45. Lisbon, Portugal: LNEC.

Donaghe, R. T., and V. H. Torrey. 1979. "Scalping and replacement effects on strength parameters of earth-rock mixtures." In Vol. 2 of *Proc. Design Parameters in Geotechnical Engineering*, 29–34. London: BGS.

French Standard. 1992. *Coefficient de fragmentabilité des matériaux rocheux*. NF P94–066. Paris: Afnor.

Gens, A., and D. M. Potts. 1988. "Critical state models in computational geomechanics." *Eng. Comput.* 5 (3): 178–197. https://doi.org/10.1108/eb023736.

Hardin, B. O. 1985. "Crushing of soil particles." *J. Geotech. Eng.* 111 (10): 1177–1192. https://doi.org/10.1061/(ASCE)0733-9410(1985)111:10(1177).

Iannacchione, A. T., and L. E. Vallejo. 2000. "Shear strength evaluation of clay-rock mixtures." In *Proc., Geo-Denver 2000*. Reston, VA: ASCE.

Jacky, J. 1948. "Pressure in silos." *Vol. 1 of 2nd ICSMFE* 103–107. London: Balkema.

JAE/LNEC (Junta Autónoma de Estradas/Laboratório Nacional de Engenharia Civil). 1991. "Via longitudinal do Algarve. Lanço Tavira-Pinheira. Ensaio de colapso." In *Proc. 053/1/9318. Outubro de 1991*. Lisbon: JAE/LNEC.

JAE/LNEC (Junta Autónoma de Estradas/Laboratório Nacional de Engenharia Civil). 1998. *Normas da junta autónoma de estradas*. Lisbon: JAE/LNEC.

Justo, J. L. 1991. "Collapse: Its importance, fundamentals and modeling." *Chap. 6 in Advances in rockfill structures*, Vol. 200 NATO ASI series, Series E: Applied sciences, 97–152. Lisbon: Kluwer Publication.

Lade, P. V., J. A. Yamamuro, and P. A. Bopp. 1996. "Significance of particle crushing in granular materials." *J. Geotech. Eng.* 122 (4): 309–316. https://doi.org/10.1061/(ASCE)0733-9410(1996)122:4(309).

Lee, K. L., and I. Farhoomand. 1967. "Compressibility and crushing of granular soils in anisotropic triaxial compression." *Can. Geotech. J.* 4 (1): 68–86. https://doi.org/10.1139/t67-012.

Lo, K. Y., and M. Roy. 1973. "Response of particulate materials at high pressures." *Soils Found.* 13 (1): 61–76. https://doi.org/10.3208/sandf1972.13.61.

Lowe, J. 1964. "Shear strength of coarse embankment dam materials." In Vol. 3 of *Proc., Int. Congress Large Dams*, 745–761. Paris: ICOLD.

Marachi, N. D., C. K. Chan, H. B. Seed, and J. M. Duncan. 1969. *Strength and deformation characteristics of rockfill materials*. Rep. No. TE 69-5. Berkeley, CA: Univ. of California.

Maranha das Neves, E. 1993. “Fills and embankments.” In Vol. 3 of *Proc., Int. Symp. Hard Soils and Soft Rocks*. Athens: A.A. Balkema.

Maranha das Neves, E. 2002. *Mecânica dos solos*, 1–323. Lisbon: Instituto Superior Técnico.

Marsal, R. 1967. “Large scale testing rockfill materials.” *J. Soil Mech. Found. Div.* 93 (2): 27–43.

Marsal, R. 1969. “Particle breakage in coarse granular soils.” In *Proc., 7th ICSFME*, 155–165. Mexico City: Sociedad Mexicana de Mecanica.

Marsal, R. 1973. “Mechanical properties of rockfill.” In *Embankment-dam engineering, casagrande volume*, 109–200. New York: Wiley.

Marsal, R. J., and F. A. Rosa. 1976. “Mechanical properties of rockfill soil mixtures.” In Vol. 1 of *Trans. 12th Int. Congress Large Dams*, 179–209. Paris: ICOLD.

Martins, F. B., L. A. Bressani, M. R. Coop, and A. V. D. Bica. 2001. “Some aspects of the compressibility behaviour of clayey sand.” *Can. Geotech. J.* 38 (6): 1177–1186. https://doi.org/10.1139/t01-048.

McDowell, G. R., and M. D. Bolton. 1998. “On the micromechanics of crushable aggregates.” *Géotechnique* 48 (5): 667–679. https://doi.org/10.1680/geot.1998.48.5.667.

McDowell, G. R., and J. P. Bono. 2013. “On the micro mechanics of one-dimensional normal compression.” *Géotechnique* 63 (11): 895–908. https://doi.org/10.1680/geot.12.P.041.

McDowell, G. R., and O. Harireche. 2002. “Discrete element modelling of yielding and normal compression of sand.” *Géotechnique* 52 (4): 299–304. https://doi.org/10.1680/geot.2002.52.4.299.

Monteiro, B., and J. Delgado Rodrigues. 1994. *Método sugerido para a determinação do ensaio de desgaste em meio húmido (slake-durability test)*. LNEC, NT 4/94–GEA/DG. Lisbon, Portugal: Laboratório Nacional de Engenharia Civil (LNEC).

Murphy, D. J. 1970. “Soils and rocks: Composition, confining level and strength.” Ph.D dissertation, Duke Univ.

Naylor, D. J., E. Maranha das Neves, D. Mattar, and A. Veiga Pinto. 1986. “Prediction of construction performance of Beliche dam.” *Géotechnique* 36 (3): 359–376. https://doi.org/10.1680/geot.1986.36.3.359.

Oldecop, L. A., and E. E. Alonso. 2001. “A model for rockfill compressibility.” *Géotechnique* 51 (2): 127–139. https://doi.org/10.1680/geot.2001.51.2.127.

Oldecop, L. A., and E. E. Alonso. 2007. “Theoretical investigation of the time dependent behavior of rockfill.” *Géotechnique* 57 (3): 289–301. https://doi.org/10.1680/geot.2007.57.3.289.

Pardo, S. F. 2006. “Structural behavior of Beliche earth-rock dam after rehabilitation works.” In *Proc., 22nd Congress of Large Dams*. Barcelona, Spain: ICOLD.

Portuguese Standard. 2002. *Ensaios das propriedades mecânicas e físicas dos agregados. Parte 2: Métodos para determinação da resistência à fragmentação*. NP EN 1097-2. Caparica, Portugal: Instituto Português Da Qualidade (IPQ).

Roscoe, K. H., A. N. Schofield, and C. P. Wroth. 1958. “On the yielding of soils.” *Géotechnique* 8 (1): 22–53. https://doi.org/10.1680/geot.1958.8.1.22.

Santucci, F., F. Silvestri, and F. Vinale. 1998. “The influence of compaction on the mechanical behavior of a silty sand.” *Soils Found.* 38 (4): 41–56. https://doi.org/10.3208/sandf.38.4_41.

Schofield, A. N., and C. P. Wroth. 1968. *Critical state soil mechanics*. London: McGraw-Hill.

Terzaghi, K. 1960. “Discussion on Salt Springs and Lower Bear River dams.” *Trans.* 125 (2): 139–148.

Vallejo, L. E., and R. Mawby. 2000. “Porosity influence on the shear strength of granular material-clay mixtures.” *Eng. Geol.* 58 (2): 125–136. https://doi.org/10.1016/S0013-7952(00)00051-X.

Vallerga, B. A., H. B. Seed, C. L. Monismith, and R. S. Cooper. 1957. *Effect of shape, size and surface roughness of aggregate particles on the strength of granular materials*. Special Technical Publication No. 212. West Conshohocken, PA: ASTM.

Veiga Pinto, A. 1983. *Previsão do comportamento estrutural de barragens de enrocamento. Tese para obtenção do grau de especialista*. West Conshohocken, PA: LNEC.

Veiga Pinto, A., and M. Prates. 1997. “Aterros de estradas. Projeto, construção e comportamento.” In *6° Congresso Nacional de Geotecnia*, 821–833. Lisbon: IST.

Wang, Y., X. Li, and B. Zheng. 2017. “Stress-strain behavior of soil-rock mixture at medium strain rates—Response to seismic dynamic loading.” *Soil Dyn. Earthquake Eng.* 93 (Feb): 7–17. https://doi.org/10.1016/j.soildyn.2016.10.020.

Xu, M., E. Song, and G. Cao. 2009. “Compressibility of broken rock-fine grain soil mixture.” *Geomech. Eng.* 1 (2): 169–178. https://doi.org/10.12989/gae.2009.1.2.169.

Yamamuro, J. A., and P. V. Lade. 1993. “Effects of strain rate on instability of granular soils.” *Geotech. Test. J.* 16 (3): 304–313. https://doi.org/10.1520/GTJ10051J.

Zeller, J., and R. Wulliman. 1957. “The shear strength of shell material for Goschenalp dam, Switzerland.” In Vol. 2 of *Proc. 4th Conf. Soil Mechanics and Foundation Engineering*, 399–404. London: Butterworths.

Zhang, Z., W. Xu, W. Xia, and H. Zhang. 2016. “Large-scale in-situ test for mechanical characterization of soil-rock mixture used in an embankment dam.” *Int. J. Rock Mech. Min. Sci.* 86 (Jul): 317–322. https://doi.org/10.1016/j.ijrmms.2015.04.001.